Frequency Shifting and Asymmetry in Infrared Bands of Stressed Polymers

Robert S. Bretzlaff and Richard P. Wool*

Department of Metallurgy and Mining Engineering, University of Illinois, Urbana, Illinois 61801. *Received November 2, 1982*

ABSTRACT: The effect of stress and temperature on infrared frequency shifting and band asymmetry in polymers is investigated. Valence coordinate deformation of individual polypropylene chains accounts for the observed frequency shifting in samples of oriented isotactic polypropylene. Each chain may be modeled as a one-dimensional anharmonic system, whose wave functions and energies are obtained in the quasi-harmonic approximation. The theoretical stress-induced frequency shifting coefficient is related to the Grüneisen parameter and is expressed by $\alpha_c = -\alpha_0 - CT_{osc}$, where α_0 and C are positive constants and T_{osc} is the temperature of the oscillators in equilibrium with the radiation field. Two mechanisms of band broadening are considered: The first is due to the presence of an average interchain perturbing force. The second is due to the existence of anisotropic crystal field forces. Each description predicts symmetric broadening. Therefore, the development of an observable asymmetry in a stressed infrared band may be associated with a nonuniform molecular stress distribution. Only the crystal field broadening mechanism, however, is consistent with the assumptions required for calculation of the linear $\alpha_c(T)$ relation, which agrees well with experiments on oriented polypropylene. The anisotropic broadening mechanism is also investigated for oriented polyethylene.

Introduction

The study of the vibrational spectra of mechanically stressed polymers can be used to obtain significant information on single- and multichain deformation processes. In studies[1,2] of highly oriented isotactic polypropylene it was noted that all the peak frequency shifts were found, with one exception, to be in the direction of lower frequency. The shifts appear as a linear function of stress and can be expressed by

$$\Delta\nu_\sigma = \nu(\sigma) - \nu(0) = \alpha_x\sigma \tag{1a}$$

where $\Delta\nu_\sigma$ is the mechanically induced peak frequency shift, α_x is the mechanically induced frequency shifting coefficient at constant temperature T, and σ is the applied uniaxial stress. The decrease of virtually all the stressed polypropylene frequencies has been interpreted[3] as showing that the anharmonicity of the carbon–carbon potential energy function must be considered in the spectroscopic analysis of polypropylene chains.

The vibrational spectra of thermally stressed polymers will be shown in the following sections to have peak frequency shifts that are fundamentally related to the above and can be expressed by

$$\Delta\nu_T = \nu(T_2) - \nu(T_1) = \beta_x(T_2 - T_1) \tag{1b}$$

where $\Delta\nu_T$ is the thermally induced peak frequency shift, β_x is the thermally induced frequency shifting coefficient at constant stress σ, and T is the sample's temperature.

The mechanically induced frequency shifting coefficient α_x is a function of temperature, morphology, thermal history, and stress history.[2] These variations in α_x describe a variable sensitivity of the absorption peak position to the externally applied stress, resulting from a variable nonuniform distribution of stress on a molecular scale. For highly oriented systems this molecular stress distribution function is relatively narrow, such that the sample tensile modulus E_x and the sample α_x approach the corresponding single-chain values E_c and α_c, respectively.

Even for relatively narrow distributions, the effect of nonuniform molecular stresses can be observed on the IR bands of highly oriented isotactic polypropylene, whose spectrum is shown in Figure 1. Figure 2 shows the 1168-cm^{-1}, parallel-polarized band obtained by a Nicolet 170 SX FT IR. Successive uniaxial stress levels from 0 to 22 kg/mm^2 applied in the sample's orientation direction produce not only a progression of peak shifts but also an increasing asymmetric wing. Figure 3 emphasizes this asymmetric wing by plotting unstressed (A), intermediately stressed (B), and highly stressed (C) bands in ultraoriented isotactic polypropylene, but with each band peak coinciding. Figure 3 shows both the band broadening and the larger shape change on the low-frequency side of the band. The amount of shape change common to both sides of the band, due in part to conformational defects,[4] extensional orientation,[5] and sample thinning, is neglected in this treatment. This is justified for small deformations in highly oriented systems, where eq 1a is obeyed. Deconvolution[6] of a typical band confirms that the significant shape changes are on the low-energy side. The difference spectra between curves in Figure 2, on the other hand, would not be useful for distinguishing the asymmetric wing, because the large derivative shape caused by the peak frequency shift[7] would swamp out the small band asymmetry.

Several investigators[1,2,6,8–10] have argued that this stress-induced wing indicates that some of the elementary oscillators in the sample have been shifted in frequency more than others. Hence, the wing is a measure of the number of "overstressed" chains. The distribution of chain segments among different stress levels, or molecular stress distribution, arises from the existence of molecular entanglements or inhomogeneous microstructures. One value of applied stress therefore causes a microstress distribution and an asymmetric wing which are sensitive to changes in the morphology, temperature, and deformation rate. This molecular stress distribution function is an important quantity, because, for example, its time evolution can determine stress relaxation moduli or creep compliances, which, in turn, determine the mechanical and fracture response of a viscoelastic material.[2]

One way to determine the molecular stress distribution is to consider a polarized infrared band, $D(\nu)$, which may be described as the convolution integral of an elementary band shape contribution, $U(\nu)$, times an oscillator number distribution, $F(\nu)$, given by

$$D(\nu) = \int_{-\infty}^{\infty} F(\xi)U(\nu - \xi)\, d\xi \tag{2}$$

where ξ is a dummy variable on the ν axis. $F(\nu)$ may be determined by solving the integral equation (2). Of course, there can be a different oscillator number distribution for each chain segment orientation, the net effect of which is $F(\nu)$. No attempt is made here to distinguish these con-

0024-9297/83/2216-1907$01.50/0

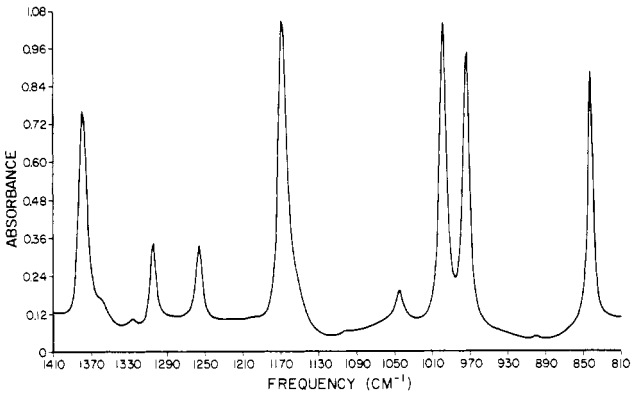

Figure 1. Survey spectrum of highly oriented isotactic polypropylene obtained at 4-cm^{-1} resolution with parallel polarization.

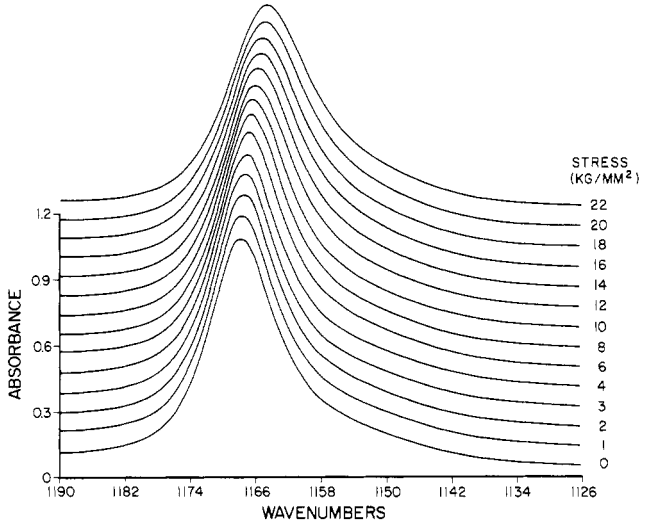

Figure 2. Parallel-polarized 1168-cm^{-1} band of highly oriented isotactic polypropylene shown at successive stress levels. The average stress application rate was 0.5 (kg/mm^2)/min. The spectra were obtained at 4-cm^{-1} resolution, and the profiles of successive levels were vertically offset by 0.09 absorbance unit.

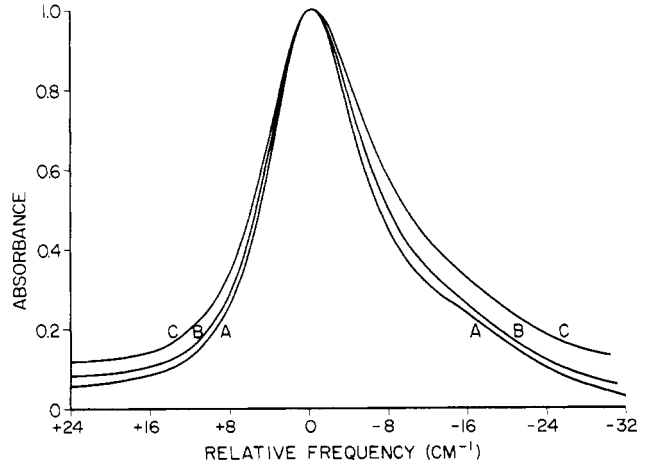

Figure 3. Unstressed (A), intermediately stressed (B), and highly stressed (C) absorption bands in highly oriented isotactic polypropylene, with each band shifted so that its peak position coincides with the others. This highlights the greater amount of low-frequency shape change.

tributions. Furthermore, $F(\nu)$ will depend on which band is chosen for $D(\nu)$, because, for example, a side-group-dominated band may be less affected by stress than a band dominated by skeletal carbon–carbon axial stretching. $F(\nu)$ can be converted to $F(\sigma)$ by using eq 1a, in which α_x is extrapolated to the corresponding value for a single chain, α_c. In this paper we examine several spectroscopic effects of stress- and temperature-dependent microscopic processes occurring within one chain or between groups of chains which influence frequency shifts and band asymmetry.

In the absence of radiation, the average interchain force on each oscillator establishes thermal equilibrium. Phonon-mediated transitions occur to ensure that the Boltzmann distribution of oscillators among levels is maintained corresponding to the ambient teperature, T_{amb}. In addition, if there are anisotropic interchain forces acting on each oscillator, the principal energy levels show crystal field splitting by a small amount (compared to kT) at room temperature. Thermal fluctuations cause oscillators to have (nearly) randomly varying lifetimes in each energy sublevel.

In the presence of radiation, the average (intrachain) quantum number and, hence, the oscillator temperature, T_{osc}, of the oscillators in each chain increases until the rate of absorbing radiation energy equals the rate of emitting thermal energy to neighboring chains and, eventually, to the sample's environment. If this interchain energy transfer occurs rapidly (strongly damped case), then $T_{osc} \approx T_{amb}$, the infrared bands are very broad, and the vast majority of the oscillators remain in the ground state. If this interchain energy transfer occurs slowly (weakly damped case), then $T_{osc} > T_{amb}$, and the infrared bands are relatively narrow. A significant fraction of the oscillators has very high quantum numbers. Depending on the average lifetime in each crystal field state, there may be an independent contribution to the observed broadening. This effect has been termed Markovian broadening by Kubo,[11] since it may be analyzed in terms of randomly varying lifetimes.

In this analysis the sample is considered to consist of large crystalline regions of common orientation containing mostly extended chains. There are smaller intervening regions of amorphous chains. The primary effect of an applied uniaxial stress is to establish a most common stress level on the great majority of the crystalline regions. The resonant frequencies of the chains are (almost always) reduced by the resulting intramolecular deformation. The secondary effect of the applied stress is to set up a distribution of larger stress levels for a small minority of the crystalline regions due to the entangled, inhomogeneous nature of the amorphous interconnecting chains. The chains in the overstressed crystalline regions will be deformed more, and the resonant frequencies shifted more, leading to the asymmetric wing.

In this paper representative experimental data will be provided and the peak frequency shifting analyzed as a function of stress and temperature in terms of the quasi-harmonic approximation for one-dimensional anharmonic model chains. The average interchain interaction will be introduced by way of one parameter, γ_0, related to the breadth of an infrared band, and the corresponding oscillator temperature will be analyzed. The Markovian broadening of infrared bands will be introduced by means of one parameter, Z, the average lifetime parameter for the crystal field split states. The following will be shown: (1) The quasi-harmonic approximation for a one-dimensional anharmonic model chain allows the interpretation of an anharmonic system as being harmonic but with a variable (stress- and temperature-dependent) spring constant. (2) At all physically reasonable T_{osc}, all significantly populated quantum states of the one-dimensional anharmonic model chain are equally spaced in energy. (3) Previous $\alpha_x = \alpha_x(T)$ data require T_{osc} to be high ($kT_{osc} \gg \hbar\omega_0$ = resonant en-

ergy). The γ_0 bandwidth parameter is correspondingly too small to describe the observed infrared bands. However, the parameter Z can be chosen so as to account for the observed width, implying that the Markovian broadening is the dominant mechanism of infrared band broadening in highly oriented isotactic polypropylene. (4) Consistent with the predominance of Markovian broadening, it is predicted that if Z is decreased by lowering T_{amb} sufficiently, then each crystalline band shown in Figure 1 will exhibit crystal field splitting, provided that there is sufficient spectral resolution, as discussed below. (The crystal field splitting of energy levels only broadens, but does not shift, the peaks at sufficiently high Z values,[11] which evidently occur at room temperature.[5] The calculated broadening and temperature effects are symmetric. Thus, previous interpretations of the asymmetric wing on stressed infrared bands as due to overstress should remain viable.

Experimental Section

Sample Characterization and Experimental Procedure. Samples of highly oriented isotactic polypropylene were characterized and provided by R. Desper.[12] The film thickness is 35.6 μm. The optical birefringence as determined by a polarizing microscope with a Berek compensator is 140×10^{-4}. The tensile modulus at 0.5 (kg/mm^2)/min stress rate is 372 kg/mm^2. The film has Hermans orientation functions, as determined by X-ray measurements, f(crystal) = 0.9854, f(amorphous) = 0.40, and f(average) = 0.78.

Experiments consist of stressing a $^1/_2'' \times 3''$ sample at a constant temperature or heating a sample at a constant applied stress while the FT IR simultaneously acquires frequency, intensity, and measurement condition information. Stress is applied parallel to the chain orientation direction. A gold wire grid (Perkin-Elmer) polarizer was used to obtain polarized spectra such that the incident electric vector was either parallel or perpendicular to both the sample orientation axis and stretching direction.

The Nicolet 170 SX FT IR is compatible with a tensile testing system consisting of a pneumatic piston, sample grips, heatable chamber, and stress-, strain-, and temperature-monitoring devices. The stressed samples were subjected to a staircase loading history, with three spectra taken at each constant load level to verify the accuracy of the frequency determination. The spectra of the heated samples were taken during temperature scans of 1.5 K/min.

The measurement time per spectrum for these 35.6-μm films was usually about 40 s. In general, sample thickness determines this time, with the criterion being the reproducibility ($\pm$0.05 cm^{-1} or better) of the peak frequencies as determined by Nicolet's cubic-spline curve fitter operating on the digitally acquired data points. These data points have a frequency accuracy of $\pm$0.01 cm^{-1}, but the "noise" (due primarily to air currents) in each absorbance channel may easily give rise to peak frequency fluctuations in excess of $\pm$0.05 cm^{-1}. Increasing measurement time, decreasing sample thickness, and the use of a "glovebox" around the sample chamber and stress rig reduce the noise level. Increasing the resolution beyond the 4 cm^{-1} used in these experiments would result in an unacceptably large increase in the measurement time for spectra without revealing new features of bands whose full width half-maxima are in excess of 10 cm^{-1}. Thus the sensitivity of these measurements on peak frequency determination is limited not by the frequency resolution chosen but by the measurement time per spectrum necessary to suppress the noise in the digital channels.

No correction for reflectance has been attempted in these measurements, nor are the slowly varying (with stress) base lines accounted for in the cubic-spline peak-picking procedure. A spectral resolution enhancement procedure (discussed below) with base line correction capability was also employed, and no difference in $\Delta\nu(\sigma)$ was seen. Thus, these corrections are not thought to have an observable effect on the samples and experiments considered here.

At least two techniques[6,13] are quoted in the literature for obtaining $F(\nu)$ in eq 2. We implemented Ergun's technique,[13] which is the unfolding of convolution products based on the substitution of successive foldings. Required integrations are performed by Simpson's rule, with at least four points interpolated into each original (2 cm^{-1}) interval to provide a stable solution. Each band was base line corrected to go to zero at each edge of its interval, so that no jump-discontinuity problems occurred. Equation 2 becomes tractable only if it is assumed that the elementary band is independent of stress, as in ref 6. The elementary band for each series of stress levels is taken to be the normalized unstressed band obtained before application of stress. This deconvolution of a given band with respect to another is a feature of our computer code, which distinguishes it from the Fourier self-deconvolution program (IRDCON.FTN), which is available with the Nicolet software.[14,15]

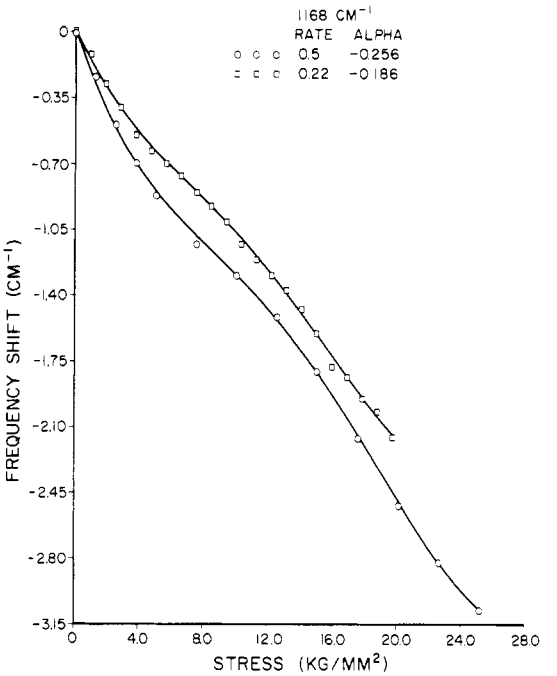

Figure 4. Typical stress-induced frequency-shifting output obtained for the 1168-cm^{-1} parallel-polarized band in highly oriented isotactic polypropylene. The 0.22 and 0.5 (kg/mm^2)/min stress rate results are shown.

Table I
Stress- and Temperature-Induced Frequency-Shifting Coefficients α_x and β_x, Respectively, for Several Bands in Highly Oriented Isotactic Polypropylene

band, cm^{-1}	α_x, cm^{-1}/(kg/mm^2) ($\pm$0.003)	β_x, cm^{-1}/K ($\pm$0.0003)
841	−0.016	−0.0014
973	−0.041	−0.0037
998	−0.011	+0.0030
1168	−0.186	−0.0238
1255	−0.002	−0.0000
1304	+0.013	−0.0054
1378	+0.001	−0.0123

Experimental Results

Examples of stress and temperature scans are shown in Figures 4 and 5. The average stress application rates for Figure 4 are 0.22 and 0.5 (kg/mm^2)/min at room temperature. The heating rate in Figure 5 is 1.5 K/min at zero applied stress. The stress scan data are least-squares curve fit to $\Delta\nu = \alpha_x\sigma + b\sigma^2 + c\sigma^3 + d\sigma^4$. The temperature scan data are least-squares curve fit to $\Delta\nu = \beta_x\Delta T$. Results for α_x (0.22 (kg/mm^2)/min) and β_x (1.5 K/min) for several bands are given in Table I. An interpretation of these shifts in terms of their "mixing" and "anharmonic" contributions is given in ref 16.

The theory of one-dimensional anharmonic chains[16] in the absence of interchain forces may easily be generalized

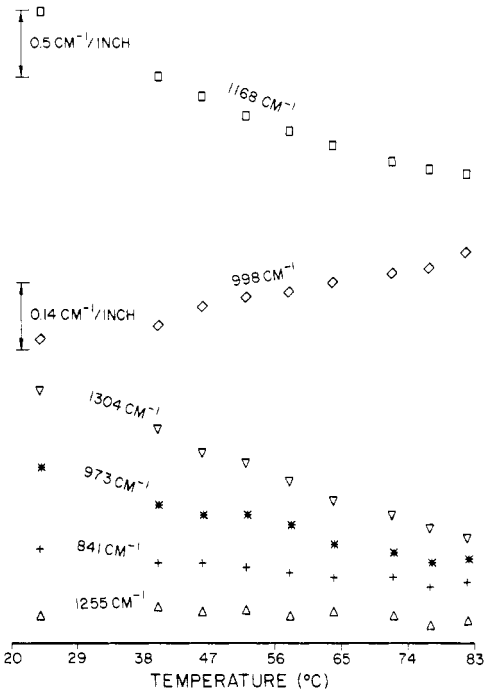

Figure 5. Typical temperature-induced frequency-shifting output obtained for the indicated parallel-polarized bands in highly oriented isotactic polypropylene. The measurements were taken during heating at 1.5 K/min.

to account for the experimental effects summarized by eq 1a and 1b:

$$\Delta\nu = \alpha_c \Delta f_c + \beta_c \Delta T \tag{3a}$$

where $\Delta\nu = \nu(f_c + \Delta f_c, T + \Delta T) - \nu(f_c, T)$ = frequency shift, f_c is the force on a single chain, T is the temperature, and α_c and β_c are the single-chain stress and temperature coefficients of frequency shifting, respectively. It has been shown[16] that (in the high-temperature limit, to be discussed below)

$$\alpha_c = -\alpha_0 - CT \tag{3b}$$

where α_0 and C are positive constants. If $\nu(f_c, T)$ has continuous partial derivatives, a Maxwell-type crossing relation gives

$$\beta_c = -\beta_0 - Cf_c \tag{3c}$$

where β_0 is another constant. Temperature-scan data as in Figure 5 are being generated[17] at different f_c levels to check whether or not the constant "C" is the same in both eq 3b and eq 3c, as predicted by the theory of one-dimensional anharmonic chains in the absence of interchain forces.

The survey spectrum of several peaks in highly oriented isotactic polypropylene is shown in Figure 1 and the corresponding self-deconvoluted bands are shown in Figure 6. If an infinite number of interpolated points and an infinite computing time were possible, Figure 6 would be, in principle, a series of delta functions. The actual finite number of points and limited computing time cause a broadening of the peak and the development of side lobes, which obscure the development of the asymmetric wing. Thus, a lthough Ergun's method does an excellent job of spectral resolution enhancement, it cannot sensitively determine $F(\nu)$ in eq 2. In the future, Kosobukin's method[6] of deconvolution and others will be implemented in order to find $F(\nu)$.

Ergun's deconvolution procedure, however, did allow us to check the peak frequency shifting results by running a special peak picker on the distribution functions. The

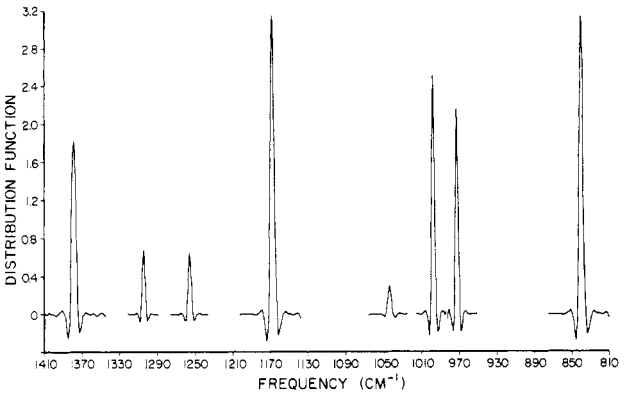

Figure 6. Self-deconvoluted spectra corresponding to Figure 1 obtained with Ergun's technique.

results were in excellent agreement with the cubic-spline peak picker operating on the original absorption bands, thereby confirming that base line corrections are not important when finding $\Delta\nu(\sigma)$ for these samples and that the absorption peak shift is in correspondence with the peak in the stress distribution function. In the next section, we investigate the spectroscopic and theoretical aspects of the observed frequency shifts and band asymmetry.

Theoretical Analysis of a One-Dimensional Chain

Validity of the Quasi-harmonic Approximation. In a recent paper,[16] Bretzlaff and Wool analyzed the effect of temperature on vibrational frequency shifts in mechanically stressed polymer chains. A single chain was modeled as a weakly coupled,[18] one-dimensional series of anharmonic diatomic oscillators. For one such oscillator, the vibrational potential $V(x)$ was written as

$$V(x) = \frac{1}{2}K_0x^2 + \frac{1}{6}g_0x^3 + \frac{1}{24}h_0x^4 \tag{4a}$$

where x is the relative displacement of the mass points in the diatomic oscillator and K_0, g_0, and h_0 are the harmonic, cubic, and quartic bonding parameters, respectively.

In considering the effect of finite temperature or external stress on a system described by eq 4a, the total effective potential $V_{tot}(x)$ may be written as

$$V_{tot}(x) = \frac{1}{2}K_0x^2 + \frac{1}{6}g_0x^3 + \frac{1}{24}h_0x^4 - \left[K_0x_1 + \frac{1}{2}g_0x_1^2 + \frac{1}{6}h_0x_1^3\right]x \tag{4b}$$

Figure 7 shos the potential energy change that occurs upon increasing the stress or temperature on a system modeled as a weakly coupled, one-dimensional series of anharmonic diatomic oscillators. Parabola A in Figure 7 corresponds to eq 4a, where $x = 0$ is the average relative displacement of the mass points in an unstressed oscillator. Parabola B in Figure 7 shows that the effect of increasing temperature or stress (eq 4b) is to increase the equilibrium value $x = x^1 > 0$, corresponding to thermal expansion[16] or to the mechanical deformation of the chain in the present analysis. In either case, the increased spacing between mass points corresponds to weaker bonding ($g_0 < 0$) by the anharmonic potential energy and to a reduced energy level separation for parabola B in Figure 7. Detailed formulas for this effect may be derived by first expanding eq 4b around x_1 to give

$$V_{tot}(x) = V_0 + \frac{1}{2}\left[K_0 + g_0x_1 + \frac{1}{2}h_0x_1^2\right](x - x_1)^2 + \frac{1}{6}[g_0 + h_0x_1](x - x_1)^3 + \frac{1}{24}h_0(x - x_1)^4 \tag{4c}$$

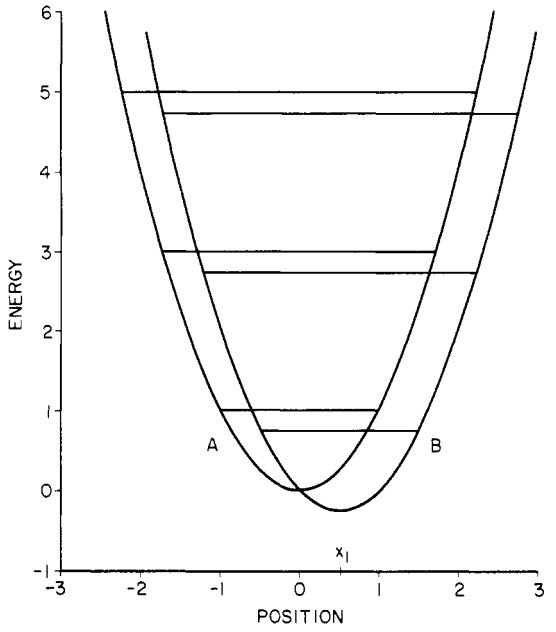

Figure 7. Unstressed (A) and stressed (B) potential energy functions for the model chain parameterized according to the example developed in the text drawn to scale. The abscissa is given in units of classical turning radius, and the ordinate in units of ground-state energy.

where V_0 is a constant. In terms of the notation in ref 16, $x_1 = \Delta l$, and x_1 is a function of the temperature T and the applied stress σ. Thus eq 4c may be considered as $V_{tot}(x,x_1) = V_{tot}(x,T,\sigma)$.

The quasi-harmonic approximation[16,20,21] calls for the retention of only the leading correction to K_0 and of only the largest cubic and quartic terms in eq 4c to form the quasi-harmonic potential energy $V_{qh}(x)$:

$$V_{qh}(x) = \frac{1}{2}[K_0 + g_0x_1](x - x_1)^2 + \frac{1}{6}g_0(x - x_1)^3 + \frac{1}{24}h_0(x - x_1)^4 \quad (4d)$$

Equation 4d allows the frequency to be calculated as for a perfect harmonic oscillator with a variable (stress and temperature dependent) spring constant. The cubic and quartic terms are used in the calculations of the thermal expansion coefficient and the specific het. The final result[16] for the given temperature dependence of the frequency shifting coefficient α_c was given previously by eq 3b. The result is in excellent qualitative agreement with the measured behavior in ultraoriented isotactic polypropylene.[16,22] The success of this one-dimensional model under the quasi-harmonic approximation indicates that not all the details pertaining to polypropylene chains need be considered on this level of description.

Quasi-harmonic Wave Functions and Energy Levels. For our model of a weakly coupled,[18] one-dimensional series anharmonic diatomic oscillators, it is desired to obtain the wave functions and energy levels for both the unstressed (eq 4a) and stressed (eq 4d) cases.

Unstressed Case. For a one-dimensional system obeying eq 4a, Rayleigh–Schroedinger nondegenerate perturbation theory can be applied as in ref 23 and 24:

$$|\phi_p\rangle = |p\rangle - \sum_{n\neq p} \frac{H_{np}^{(3)}|n\rangle}{E_n^0 - E_p^0} \quad (5a)$$

$$E_p = E_p^0 + H_{pp}^{(4)} - \sum_{m\neq p} \frac{|H_{mp}^{(3)}|^2}{E_m^0 - E_p^0} \quad (5b)$$

where $|\phi_p\rangle$ and E_p are the quasi-harmonic wave functions and energies, $|p\rangle$ and E_p^0 are the perfect harmonic wave functions and energies, and $H_{mp}^{(j)} = \langle m|H^{(j)}|p\rangle$ are the anharmonic matric elements of the jth-order terms $H^{(3)} = g_0x^3/6$ and $H^{(4)} = h_0x^4/24$. The following definitions are made: The fundamental frequency $\omega_0 = (K_0/\mu)^{1/2}$, the classical turning radius $l = (\hbar/\mu\omega_0)^{1/4}$, and the displacement $x = l(a^+ + a)/2^{1/2}$, where μ is the reduced mass of the diatomic oscillator, $\hbar$ is Planck's constant/2π, c = speed of light in vacuum, and a^+ and a are the raising and lowering operators. The calculation of the necessary matrix elements then gives the results for the wave functions and energy levels as follows:

Wave functions

$$|\phi_0\rangle = |0\rangle + \theta\left\{-\frac{1}{2}|1\rangle - \frac{1}{3(6^{1/2})}|3\rangle\right\} \quad (6a)$$

$$|\phi_1\rangle = |1\rangle + \theta\left\{\frac{1}{2}|0\rangle - 2^{1/2}|2\rangle - \frac{2^{1/2}}{3(3^{1/2})}|4\rangle\right\} \quad (6b)$$

$$|\phi_2\rangle = |2\rangle + \theta\left\{2^{1/2}|1\rangle - \frac{3(3^{1/2})}{2}|3\rangle - \frac{5^{1/2}}{3(3^{1/2})}|5\rangle\right\} \quad (6c)$$

$$|\phi_n\rangle = |n\rangle + \theta\left\{\frac{(n(n-1)(n-2))^{1/2}}{18}|n-3\rangle + \frac{n^{3/2}}{2}|n-1\rangle - \frac{(n+1)^{3/2}}{2}|n+1\rangle - \frac{((n+1)(n+2)(n+3))^{1/2}}{18}|n+3\rangle\right\} \quad (n \geq 3) \quad (6d)$$

Energy Levels

$$E_n = \hbar\omega_0\left(n + \frac{1}{2}\right) + \frac{h_0l^4}{32}(2n^2 + 2n + 1) - \frac{g_0^2l^6}{288\hbar\omega_0}(30n^2 + 30n + 11) \quad (n \geq 0) \quad (6e)$$

where

$$\theta = \frac{g_0l^3}{2(2^{1/2})\hbar\omega_0} \quad (7)$$

Note that the perfect harmonic case ($g_0 = 0$, $h_0 = 0$) implies $\theta = 0$, so that $|\phi_n\rangle = |n\rangle$ and $E_n = \hbar\omega_0(n + {}^1/_2)$, as required.

Stressed Case. The effect of stress on a system described in the quasi-harmonic approximation by eq 4d may be analyzed as above. The analysis leads to the same type of equations as eq 6a–e and eq 7 above, the only changes being in the fundamental frequency ω_0' and the classical turning radius l': $\omega_0' = ((K_0 + g_0x_1)/\mu)^{1/2}$ and $l' = (\hbar^2/(\mu(K_0 + g_0x_1)))^{1/2}$. Figure 7 shows the difference in the parabolas corresponding to eq 4a and 4d. The variable x_1 is a measure of the effect of stress and temperature on the system. The energy level spacings for these parabolas will be derived in the following sections.

Comparison with Morse Theory. The perturbation treatment of eq 4a or 4d may be checked by the use of an analytic expression for $V(x)$, which is valid for all values of x and which can be solved exactly. One such potential is the Morse potential $V^{(m)}(x)$:[25]

$$V^{(m)}(x) = C[1 - \exp(-a(x - x_1))]^2 \quad (8a)$$

$$E_n^{(m)} = \hbar\omega_0\left(n + \frac{1}{2}\right) - \frac{\hbar^2\omega_0^2}{4C}\left(n + \frac{1}{2}\right)^2 \quad (8b)$$

where $\omega_0 = (K_0/\mu)^{1/2}$ and $K_0 = 2Ca^2$, where C and a are

constants. In order to check the perturbation theory results, eq 8a may be expanded around x_1. Comparing the result to eq 4d, one observes that $g_0 = -6Ca^3$ and $h_0 = 14Ca^4$. Substituting these K_0, g_0, and h_0 values into eq 6e, it may verified that eq 8b is obtained, as required. The only difference between these solutions is that the perturbation theory quantum number n is limited by the relation $n \ll \theta^{-2}$ and differs, in general, from the finite number of bound states for the Morse potential.

Consequences of the Quasi-harmonic Approximation for Stressed Polymers

We proceed now to describe the different energy level spacings for the parabolas in Figure 7 that give rise to the stress-induced frequency shift.

The right-hand side of eq 6e contains two kinds of terms: (1) The first term contains the variable spring constant K_0 (unstressed) or $K_0 + g_0x_1$ (stressed) and is therefore the quasi-harmonic contribution to the energy. (2) The second and third terms contain the cubic and quartic perturbation energies and are therefore the so-called self-energy terms. It is desired to verify that the stress-induced quasi-harmonic shift in transition frequencies is much greater than the self-energy shift. If that is true, then the observed energy shifts will be adequately described by the quasi-harmonic contribution, i.e., by a perfect harmonic oscillator with a variable (stress and temperature dependent) spring constant.

A typical observation on highly oriented isotactic polypropylene at room temperature is that $\nu_0 = 1167$ cm^{-1} ($\hbar\omega_0 = 0.145$ eV or 0.223×10^{-12} erg) and $\Delta\nu = -0.2$ cm^{-1} at an estimated molecular deformation $x_1 = (1\%) \times$ (2-Å chemical repeat unit length) = 0.02 Å, consistent with the deformation range studied in ref 3. In this example the infrared absorption will be attributed to the appropriately parameterized, one-dimensional chain described above in order to illustrate the relationships between molecular deformation, bonding parameters, and the quasi-harmonic and self-energy contributions to frequency shifting. Physically, of course, this stress-sensitive band arises from the combined action of carbon–carbon, valence angle, and internal rotation potentials, as studied in ref 3.

On the assumption that each mass point in the model diatomic oscillator is a carbon atom, it follows from the definitions of ω_0 ($\equiv 2\pi c\nu_0$) and ω_0' ($\equiv 2\pi c\nu_0'$) that $K_0 = 4\pi^2\mu c^2\nu_0^2 = 4.85 \times 10^5$ dyn/cm and $g_0 = 2K_0\Delta\nu/\nu_0 x_1 = -8.31 \times 10^{11}$ dyn/cm^2. On the further assumption that the model potential has the same proportionality between its derivatives (evaluated at equilibrium) as does the Morse potential, it follows that $h_0 = 1.11 \times 10^{18}$ dyn/cm^3.

Comparing the definitions for the classical turning radii l and l', one obtains

$$l' = l\left(1 - \frac{g_0x_1}{4K_0}\right) \tag{9}$$

The unstressed and stressed values l and l' are 3.89×10^{-10} cm and $3.89 \times 10^{-10} \times (1.0 + 8.0 \times 10^{-5})$ cm, respectively. Furthermore, the dimensionless quantity θ (eq 7) is calculated to be -0.75×10^{-4}. Hence the perturbation treatment's validity is limited to $n \ll \theta^{-2} = 1.77 \times 10^8$. In comparison, the number of Morse states for this parameterization is approximately 10^7.

From eq 6d, it is seen that the dipole transition operator

$$p = ex = el(a^+ + a)/2^{1/2} \tag{10}$$

will connect $|\phi_n\rangle$ with the following six higher states: $\langle\phi_{n+1}|$, $\langle\phi_{n+2}|$, $\langle\phi_{n+3}|$, $\langle\phi_{n+4}|$, $\langle\phi_{n+5}|$, and $\langle\phi_{n+7}|$. The corresponding squares of the magnitudes of the transition moment vector ($\sim p^2$) stand approximately in the ratio $1{:}\theta^2n^3{:}\theta^4n^3{:}\theta^2n^3{:}\theta^4n^3{:}\theta^4n^3$. Thus the overtone transition probabilities are down by approximately 10^{-8} or more (for small n) with respect to the fundamental transition probability $n \rightarrow n + 1$. The observation of such overtones would require a thick sample with fundamental intensities in excess of 8 absorbance units before the overtone intensity would equal unity. It would seem that only in the most unusual circumstances could an overtone band be observed in systems amenable to modeling by a one-dimensional diatomic chain. We will therefore neglect overtone transitions in the following analysis.

The fundamental transition energy $\Delta R_{n,n+1}$ may be obtained from eq 6e for the transition $n \rightarrow n + 1$:

$$\Delta E_{n,n+1} = \hbar\omega_0 + \frac{h_0l^4}{8}(n + 1) - \frac{5}{24}(n + 1)\frac{g_0^2l^6}{\hbar\omega_0} \tag{11a}$$

The stress-induced shift $\delta E = \Delta E'_{n,n+1} - \Delta E_{n,n+1}$ in the transition energy is therefore

$$\delta E = \hbar(\omega_0' - \omega_0) + \frac{n + 1}{8}h_0(l'^4 - l^4) - \frac{5}{24}(n + 1)\left(\frac{g_0^2l'^6}{\hbar\omega_0'} - \frac{g_0^2l^6}{\hbar\omega_0}\right) \tag{11b}$$

Using the definitions for ω_0, ω_0', l, and l', one obtains

$$\delta E = \frac{-\hbar\omega_0|g_0|x_1}{2K_0} + \frac{n + 1}{8}h_0l^4\frac{|g_0|x_1}{K_0} - \frac{5}{12}(n + 1)\frac{g_0^2l^6}{\hbar\omega_0}\frac{|g_0|x_1}{K_0} \tag{11c}$$

Noting that $|g_0|x_1/K_0 = 3.43 \times 10^{-4}$, $h_0l^4 = 2.54 \times 10^{-20}$ erg, and $g_0l^3 = 4.89 \times 10^{-17}$ erg, it follows that

$$\delta E = -3.97 \times 10^{-17} + (n + 1)(1.09 \times 10^{-24}) - (n + 1)(1.18 \times 10^{-23}) \text{ erg} \tag{11d}$$

$$\delta\nu = -0.2 + (n + 1)(5.0 \times 10^{-9}) - (n + 1)(5.0 \times 10^{-8}) \text{ cm}^{-1} \tag{11e}$$

Even for $n \approx 10^3$, the self-energy shift is only $\approx 10^{-3}$ of the quasi-harmonic shift. It is verified below that n does not exceed 10^3. The observed transition energy shift, δE_{obsd}, is therefore completely described by the expression

$$\delta E_{obsd} = \hbar(\omega_0' - \omega_0) = \frac{-\hbar\omega_0|g_0|x_1}{2K_0} \tag{12}$$

Equation 12 states that the energy levels are equally spaced at each stress level but that the spacing depends on the stress level through x_1. This means that in the quasi-harmonic approximation, the states and energies are harmonic (to within observational limits), but with a variable (stress and temperature dependent) spring constant.

One method of describing the broadening of these resonance transitions is to summarize the effect of all interchain forces in one parameter, γ_0, which is the half-width of the observed infrared band. The possibility must be investigated, in the event of weak damping, that the radiation field could significantly populate the higher ($n \gtrsim 10^3$) levels, i.e., dramatically increase T_{osc} and allow a distribution of $n \rightarrow n + 1$ transitions at different energies. In this case, band asymmetry could arise independent of overstress. In the next section, a typical observed infrared bandwidth is assumed to originate from this effect. It will be shown that (i) $n \ll 10^3$, (ii) $T_{osc} \approx T_{amb}$, and (iii) that therefore no overstress-independent asymmetries occur.

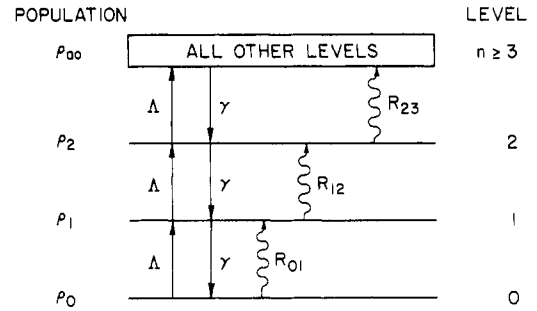

Figure 8. The three oscillator levels considered in eq 13a–c for the γ_0-broadening mechanism account for about 99.7% of the total population (at room temperature) of polymeric systems modeled by the one-dimensional anharmonic chain. Λ and γ are the nonradiative excitation and decay rates. R_{ij} are the radiative transition rates.

A second broadening mechanism considers the effects of a crystal field splitting of each of the quantum levels n into two or more closely spaced (in energy) sublevels. Such energy level splitting may or may not cause a splitting in the infrared bands, depending on the parameter Z, which is the average reciprocal lifetime of an oscillator in a sublevel. Broadening of the resonance(s), however, occurs in either case. In the section after next it will be assumed that the observed infrared broadening is primarily due to crystal field broadening. A value for the parameter Z will be inferred, as well as a general requirement on T_{osc}, which must be valid to allow crystal field broadening to predominate. Also in this case, the broadening is symmetric, and the overstress interpretation of asymmetric wings remains viable.

Finally, some experimental evidence will be presented that establishes the crystal field broadening as the predominant mechanism in our samples of ultraoriented isotactic polypropylene.

Determination of Band Broadening by an Average Interchain Force

It will be shown that (1) only the lowest few levels of a stressed or unstressed polymer modeled by a one-dimensional anharmonic chain subject to a one-parameter representation of the average interchain force have sufficient populations to play a role in infrared absorption and (2) the overtone transitions rates are inconsequential. Strictly speaking, therefore, it would be circular to perform the analysis on the basis of a population model restricted to the lowest states and to fundamental transitions only. However, in order to display the solutions in an easily understood form, only levels 0, 1, and 2 of an anharmonic system obeying eq 4a or 4d in the quasi-harmonic approximation will be considered, and it will be shown that extending the model to an arbitrary number of levels with all possible overtone transitions will not affect these solutions.

Unstressed Case. Figure 8 shows schematically the transitions modeled by the density matrix method developed in ref 26. Only the nonradiative excitation Λ and decay γ rates exist in the absence of radiation and establish thermal equilibrium at the ambient temperature T_{amb}. The populations ρ_i of the states are given by the Boltzmann distribution.

In the presence of radiation, the rate constants R_{ij} describe radiative transitions from state i to j. As first pointed out by Einstein,[27] the R_{ij} for absorption of radiation is equal in magnitude to the R_{ij} for stimulated emission of radiation. Therefore there is net absorption when the lower energy states are relatively more populated, as in systems exhibiting infrared absorption. The populations ρ_i deviate from their values in the absence of radiation and define a new (oscillator) temperature, T_{osc}. T_{osc} deviates more from T_{amb} when the incident radiation is dissipated less effectively to the sample's environment via γ_0.

The rate equations corresponding to Figure 8 for the populations during steady-state absorption of infrared energy are

$$-\Lambda\rho_0 + \gamma\rho_1 - R_{01}(\rho_0 - \rho_1) = \dot{\rho}_0 = 0 \quad (13a)$$

$$-\Lambda(\rho_1 - \rho_0) + \gamma(\rho_2 - \rho_1) - R_{12}(\rho_1 - \rho_2) + R_{01}(\rho_0 - \rho_1) = \dot{\rho}_1 = 0 \quad (13b)$$

$$-\Lambda(\rho_2 - \rho_1) + \gamma(\rho_{a_0} - \rho_2) - R_{23}(\rho_2 - \rho_{a_0}) + R_{12}(\rho_1 - \rho_2) = \dot{\rho}_2 = 0 \quad (13c)$$

where ρ_0, ρ_1, and ρ_2 are the populations of the zeroth, first, and second states and ρ_{a_0} is the population of all other states. Normalization requires $\rho_{a_0} = N_0 - \rho_0 - \rho_1 - \rho_2$, where N_0 is the total population. The following definitions are useful: $y = \Lambda/\gamma$ and $y_{ij} = R_{ij}/\gamma$. Solving by determinants, one obtains the solutions as

$$\rho_0 = (1 + y_{01})(1 + y_{12})(1 + y_{23})N_0\xi^{-1} \quad (14a)$$

$$\rho_1 = (y + y_{01})(1 + y_{12})(1 + y_{23})N_0\xi^{-1} \quad (14b)$$

$$\rho_2 = (y + y_{01})(y + y_{12})(1 + y_{23})N_0\xi^{-1} \quad (14c)$$

$$\xi = \{1 + 2y_{01} + y_{12} + y_{23} + 3y_{01}y_{12} + 2y_{01}y_{23} + y_{12}y_{23}\} + y\{1 + y_{01} + 2y_{12} + y_{23} + y_{01}y_{12} + 2y_{01}y_{23} + 3y_{12}y_{23}\} + y^2\{1 + y_{01} + y_{12} + 2y_{13}\} + y^3 \quad (14d)$$

In the absence of radiation, all $y_{ij} = 0$, and eq 14a–d reduce to the Boltzmann distribution: $\rho_i = y^i N_0\xi^{-1}$, $\xi = 1 + y^2 + y^3$, and $y = (\Lambda/\gamma) = \exp(-\hbar\omega_0/kT_{osc})$ for $i = 0$, 1, 2. At room temperature, for example, $y = \exp(-0.145$ eV$/0.025$ eV$) = 0.00303$, and 99.7% of the oscillators are in the ground state. At 400 K, $y = \exp(-0.145$ eV$/0.0345$ eV$) = 0.015$, and 98.5% of the oscillators are in the gound state.

In order to find the solutions in the presence of radiation, one must calculate the transition rates R_{ij}. In the semiclassical approximation (quantized matter, continuous electromagnetic field) these rates have been derived as follows[26] (expressed here in a slightly different notation):

$$R_{ij} = \frac{\pi^2 p_{ij}^2}{2\hbar^2} U(\omega_{ij}) L(\omega,\omega_{ij},\gamma_0) \quad (15)$$

where p_{ij} is the dipole moment connecting states i and j, $U(\omega_{ij})$ is the energy density of the infrared beam at the frequency $\omega_{ij} = \omega_i - \omega_j$, and $L(\omega,\omega_{ij},\gamma_0)$ is the normalized Lorentzian function with peak at ω_{ij} and observed half-width $\gamma_0 = \gamma - \Lambda$:

$$L(\omega,\omega_{ij},\gamma_0) = \frac{\pi^{-1}\gamma_0^{-1}}{1 + \{(\omega - \omega_{ij})/\gamma_0\}^2} \quad (16)$$

It may be shown that $U(\omega_{ij}) = (8\pi/c)S(\omega_{ij})$, where $S(\omega_{ij})$ is the magnitude of the Poynting vector of the incident radiation at frequency ω_{ij}. For a one-dimensional oscillator, the dipole moment $p_{ij} = e\langle\phi_j|x|\phi_i\rangle$, where e is the electronic charge. Therefore

$$R_{ij} = \frac{4\pi^2 e^2}{\hbar^2 c}|\langle\phi_j|x|\phi_i\rangle|^2 \left[\frac{S(\omega_{ij})}{\gamma_0}\right]\left[\frac{1}{1 + \{(\omega - \omega_{ij})/\gamma_0\}^2}\right] \quad (17)$$

The R_{ij} result may be compared to the probability per unit time, $w(\uparrow)$, for absorption by an undamped oscillator, which is given in ref 29 as

$$w(\uparrow) = \frac{4\pi^2 e^2}{\hbar^2 c} |\langle \phi_j | x | \phi_i \rangle|^2 I(\omega_{ij}) \tag{18}$$

where $I(\omega_{ij})$ is the total energy per area incident on the sample during the experiment. One observes two major differences between undamped and damped absorption: (1) There is a multiplicative Lorentz factor in eq 17. A damped oscillator has finite breadth. (2) $I(\omega_{ij})$ and hence $w(\uparrow)$ increase linearly with time, limiting the range of validity of eq 18. Only damped oscillators may exhibit steady-state absorption of energy, for which $R_{ij} \sim S(\omega_{ij})/\gamma_0$ is time independent.

For the solutions eq 14a–d we require the following resonance transition rates from eq 17:

$$R_{01} = \frac{4\pi^2}{\hbar}\left(\frac{e^2}{\hbar c}\right) l^2 \left[\frac{S}{\gamma_0}\right] \tag{19a}$$

$$R_{12} = 2R_{01} \tag{19b}$$

$$R_{23} = 3R_{01} \tag{19c}$$

where S, in this example, is due to blackbody radiation at 1500 K (default value for the Nicolet 170 SX Fourier transform infrared spectrometer) and 1167 cm^{-1}. (This assumes a lossless optical system for the sake of calculating the maximum possible effect of the radiation.) Furthermore, in the previous section we have determined $l = 3.89 \times 10^{-10}$ cm. A typical observation of the full width half-maximum of the 1167-cm^{-1} band in ultraoriented isotactic polypropylene is $2\gamma_0 \approx 16$ $cm^{-1} \approx 3 \times 10^{12}$ s^{-1}.

The Planck distribution function for blackbody radiation gives 2.86×10^{-3} $W/(cm^2\ cm^{-1})$ at 1500 K and 1167 cm^{-1}. If one considers all the radiation within two full width half-maxima as contributing to the ω_{ij} absorption, then $\Delta'\nu = 4\gamma_0 \approx 32$ cm^{-1}. Consequently, $S = 9.15 \times 10^{-2}$ W/cm^2.

Since $\gamma_0 = \gamma - \Lambda$ and $\Lambda/\gamma = \exp(-\hbar\omega_0/kT)$, $2\gamma \approx 2\gamma_0 \approx 3 \times 10^{12}$ s^{-1}. The final resuls for R_{01}, R_{12}, and R_{23} are 25, 50, and 75 s^{-1}, respectively. Hence, using $y_{ij} = R_{ij}/\gamma$, one obtains

$$y_{ij} \leq 10^{-10} \qquad i, j = 0, 1, 2 \tag{20}$$

Thus, all the radiation-dependent factors y_{ij} in eq 14a–d are negligible and the Boltzmann distribution $\rho_i = y^i N_0 \xi^{-1}$ represents the system for either unradiated or radiated sample; i.e., there is no observable deviation of T_{osc} from T_{amb}.

Stressed Case. The only difference in the solutions given by eq 14a–d would be the presence of ω_0' instead of ω_0, but the slight change involved makes no appreciable difference in the Boltzmann factor y. It is still true that $\gamma_0 \geq 10^{10} \times R_{ij}$ and $y_{ij} \leq 10^{-10}$. Therefore there is no observable deviation of T_{osc} from T_{amb}.

Extension of Model to Additional Levels. The rate equations (13a–c) would certainly become much more complicated if the five overtone transition rates were added to each level and if more levels were considered. However, in the range of validity of the one-dimensional anharmonic chain, the overtone rates cannot exceed the fundamental transition rates. All the R_{ij} will still be on the order of 10^{-10} times the damping rate γ_0. Hence there is no mechanism by which higher states may be populated, and it cannot be anticipated that the consideration of more states would change this. The solutions given by eq 14a–d ($y_{ij} = 0$) are expected to completely describe the real populations in either the presence or absence of radiation.

With the γ_0-broadening mechanism, only small n levels are populated, $T_{osc} \approx T_{amb}$, and since all levels with $n \leq 10^3$ are equally spaced, the application of a uniform microstress cannot result in band asymmetry. Band asymmetry can develop with a nonuniform molecular stress distribution.

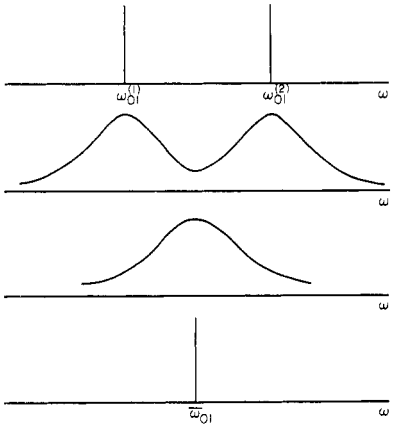

Figure 9. Crystal field splitting results in an independent Z-broadening mechanism for polymer resonance frequencies modeled by the one-dimensional anharmonic chain. Z is the average reciprocal lifetime of an oscillator in one of the crystal field sublevels, r. n is the principal (intrachain) quantum number. (a) $Z = 0$: $nr \rightarrow (n+1)r$ and $nr' \rightarrow (n+1)r'$ give rise to two sharp lines. (b) $Z > 0$: Each ground state contributes to each absorption, with the broadening shown. (c) $Z \gg 0$: More rapid state switching results in coalescence of the original resonances. (d) $Z \rightarrow \infty$: The random state switching occurs so rapidly that a sharp "average" line arises.

Determination of Band Broadening by Crystal Field Forces

Suppose that anisotropic interchain forces act on a given oscillator to produce r states, closely spaced in energy, for each intrachain quantum number n. An example of this ($r = 2$) is the 720/730-cm^{-1} polyethylene CH_2 rocking mode splitting. Analyzing the broadening of the $n = 0$ to $n = 1$ resonance frequencies, $\omega_{01}^{(1)} \neq \omega_{01}^{(2)}$, requires more than a superposition of two independent processes as outlined in the previous section. An oscillator in one of the ground-state sublevels may be abruptly "bumped" into the other by a small thermal fluctuation, since the sublevels are split by ~0.001 eV and $kT \sim 0.025$ eV at room temperature. Thus, both ground-state sublevel populations contribute to each absorption at $\omega_{01}^{(1)}$ and $\omega_{01}^{(2)}$.

Kubo[11] has analyzed this problem in another context for general r and for the special case $r = 2$. An oscillator stays in one sublevel for some time and then changes suddenly to another sublevel. The γ_0-broadening effect is neglected in this analysis of the so-called Markovian broadening. For the $r = 2$ case, let the sublevel lifetimes be $1/z^{(1)}$ and $1/z^{(2)}$. The equilibrium probabilities of finding an oscillator in a given sublevel are $P_0^{(1)} = z^{(1)}/Z$ and $P_0^{(2)} = z^{(2)}/Z$, where the reciprocal lifetime parameter $Z = z^{(1)} + z^{(2)}$. The absorption band $D(\omega)$ is calculated as

$$D(\omega) = Z\frac{P_0^{(1)}P_0^{(2)}}{\pi}\left[\frac{(\omega_{01}^{(1)} - \omega_{01}^{(2)})^2}{(\omega - \omega_{01}^{(1)})^2(\omega - \omega_{01}^{(2)})^2 + Z^2(\omega - \bar{\omega}_{01})^2}\right] \tag{21}$$

where $\bar{\omega}_{01} = P_0^{(1)}\omega_{01}^{(1)} + P_0^{(2)}\omega_{01}^{(2)}$. The results are shown schematically in Figure 9. The important points are the following: (1) If the sublevel lifetimes are infinite ($Z = 0$), then two sharp resonances occur independently of each other at $\omega_{01}^{(1)} \neq \omega_{01}^{(2)}$ as shown in Figure 9a. (2) For finite but large lifetimes, the sublevel-switching process results in two broadened peaks around $\omega_{01}^{(1)}$ and $\omega_{01}^{(2)}$ (Figure 9b).

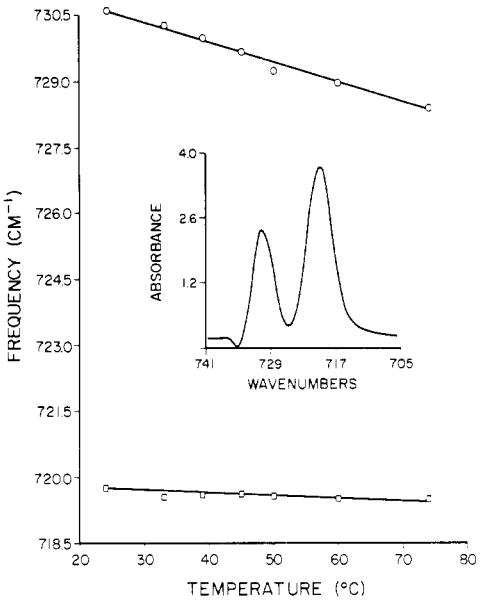

Figure 10. The convergence of the 720/730-cm^{-1} CH_2 rocking doublet in oriented polyethylene heated at 1.5 K/min is consistent with the Z-broadening mechanism. The inset shows the polyethylene spectrum, which was treated by IRDCON analysis to minimize band overlap problems.

(3) For short lifetimes in each sublevel there results one broadened peak at an average frequency $\bar{\omega}_{01}$ (Figure 9c). (4) For infinitely fast sublevel switching ($Z \rightarrow \infty$) there is a single sharp line at the average frequency $\bar{\omega}_{01}$ (Figure 9d). The complete description of the Kubo effect would be more complicated than eq 21 if the particular crystal field defines a number $r > 2$ of sublevels.

If Markovian broadening is the dominant effect, then in systems with closely spaced chains, such as PE crystals, the sublevel switching at room temperature may be slow enough to produce the 720/730-cm^{-1} CH_2 rocking doublet. Increasing the temperature in this system would be expected to decrease the crystal field forces, to increase the switching speed (Z), and to therefore reduce the observed separation between the peaks. This is just what is seen in the temperature-scan data for PE shown in Figure 10. These peaks were spectral-resolution enhanced with the program IRDCON.FTN as discussed in ref 14 and 15. There is a convergent trend in the doublet frequencies; that is, the 730-cm^{-1} slope (-4.44×10^{-2} °C^{-1}) is greater than the 720-cm^{-1} slope (-6.04×10^{-3} °C^{-1}). The convergence is not symmetric because (i) there is competing intrachain frequency shifting, (ii) the original peak absorbances are not equal, and (iii) there is preferential thermal expansion along the a axis.[31] There is an extrapolated point of intersection at 306 °C. Of course, the orthorhombic phase melts near 135 °C, so the 306 °C value only refers to a hypothetical orthorhombic state in which no splitting would occur, even at infinite spectral resolution. For finite spectral resolution, effective coalescence of the doublet may occur at a substantially lower temperature.

This convergence of the PE CH_2 rocking frequencies correlates well with the results of X-ray crystal lattice parameter measurements.[30] The a axis expands relatively rapidly with increasing temperature, while the b axis remains almost constant. It has been shown[31] that the 730- and 720-cm^{-1} polarizations are along the a and b axes, respectively. Therefore, relatively rapid temperature variations of lattice parameters and associated peak absorption frequencies coincide. In Kubo's theory, an increasing switching rate would be expected to occur concomitantly with a preferential thermal expansion that reduces the anisotropy of the crystal field. In the limit when thermal expansion eliminates anisotropic forces, the original crystal structure must by hypothesis also disappear. In that limit, only one single-chain resonance absorption frequency remains, possibly γ_0 broadened by residual isotropic forces.

In systems with more distantly spaced chains, such as PP crystals, the sublevel switching at room temperature may be fast enough that only single peaks are observed for each resonance absorption. For the observed PP bands to be described by eq 21, then Z = half-width = 10^{12} s^{-1} as determined previously. We are not aware of standards of comparison for this value, because typical analyses of "lifetime broadening" apply to excited electronic or nuclear states. In order for the γ_0 broadening to be negligible, $\gamma_0 \rightarrow 0$ and $T_{osc} \gg T_{amb}$. There is no way to tell from Z-broadened data exactly what T_{osc} is, but if one assumes $T_{osc} \approx 100T_{amb}$, then $\hbar\omega_0 = 0.145$ eV $> kT_{amb} = 0.025$ eV leads to $\hbar\omega_0 = 0.145$ eV $\ll kT_{osc} = 2.5$ eV. In that case, the $n = 100$ state would still have only 0.3% of the total population. An experimental check on the validity of this model for highly oriented isotactic polypropylene would be the measurement of the spectrum at cryogenic temperatures.[32] Then Z would be reduced, and splitting of the crystalline peaks should be observable in the infrared spectrum, provided that there is adequate spectral resolution, as discussed in ref 14 and 15.

With the Z-broadening mechanism, only $n \lesssim 100$ levels are populated, and since all levels with $n \leq 10^3$ are equally spaced, the application of a uniform microstress cannot result in band asymmetry.

Band Broadening and the Frequency-Shifting Coefficient α_c

It has been previously shown[16] that, in one dimension, the frequency-shifting coefficient for a single chain, α_c, can be described by

$$\alpha_c = -\alpha l \nu / c_v \tag{22a}$$

where

$$\alpha = \frac{-g_s}{2K_s K_w l_0}\left(\frac{\partial \bar{E}}{\partial T}\right)_l \tag{22b}$$

and

$$c_v \equiv (\partial \bar{E}/\partial T)_l \tag{22c}$$

in which the thermal expression coefficient, c_v, is the specific heat at constant "volume" (length), l_0 and l are the unstressed and stressed lengths of the diatomic cell, respectively, ν_0 and ν are the unstressed and stressed frequencies, respectively, K and g are defined in eq 4a, where the subscripts s and w now refer to the strong and weak springs in the diatomic cell, respectively, $\bar{E}$ is the average oscillator energy, and T is the "microscopic" parameter T_{osc}. Noting the exact cancellation of $(\partial \bar{E}/\partial T)_l$ and the definitions $l = l_0(1 + \alpha T)$ and $\nu = \nu_0(1 + g_s \alpha T l_0/K_s)$,[1/2], one obtains at any temeprature

$$\alpha_c = \frac{-|g_s|\nu_0}{2K_s K_w}\left[1 + \alpha T\left(1 + \frac{g_s l_0}{2K_s}\right)\right] \tag{22d}$$

Note that in ref 16, the $\bar{E}$ in the high-temperature α formula inadvertantly omitted the anharmonic terms, which were correctly deduced in the c_v result. Therefore, the $(\partial \bar{E}/\partial T)_l$ cancellation was not exact and the last term in eq 24c in ref 16 is incorrect, although it is negligible in any event. The important point is that eq 22d above is valid in any temperature regime. Now if the high-temperature

limit $kT \gg \hbar\omega_0$ is assumed as in ref 16 and the last (small) term ignored, then

$$\alpha_c = \frac{-|g_s|\nu_0}{2K_sK_w}\left[1 + \frac{|g_s|kT}{2K_sK_w l_0}\right] \tag{23}$$

and the high-temperature form $\alpha_c = -\alpha_0 - CT$ is recovered, where α_0 and C are positive constants. Near $T = 0$, the well-known $\alpha \sim (\partial\bar{E}/\partial T)_l \sim T^3$ relation[33] gives

$$\alpha_c = \frac{-|g_s|\nu_0}{2K_sK_w}\left[1 + \frac{V\pi^2|g_s|(kT)^4}{5K_sK_w l_0(\hbar c)^3}\right] \tag{24a}$$

or

$$\alpha_c = -\alpha_0 - C_L T^4 \tag{24b}$$

where α_c and C_L are appropriately defined positive constants and V is the volume of the unit cell. The interesting result is that the linear behavior at high temperature may not be extrapolated to low temperature, where a T^4 relation obtains. The intercept α_0 is, however, the same.

It has been observed[16,22] that α_c for highly oriented isotactic polypropylene is linear with ambient temperature from 200 to 400 K. That implies that the corresponding T_{osc} must be high ($kT_{osc} \gg \hbar\omega_0$). This result is incompatible with the results of the γ_0-broadening mechanism due to a hypothesized average interchain force.

On the other hand, if the Z-broadening mechanism due to a hypothesized crystal field splitting of energy levels is assumed, then Z may be chosen ($Z \approx 10^{12}$ s^{-1}) to match the observed broadening. Since γ_0 may be consistently assumed to be small, it is allowable for $kT_{osc} \gg \hbar\omega_0 \doteq 0.145$ eV $> kT_{amb} \doteq 0.025$ eV, and the observed $\alpha_c(T)$ behavior would result.

Of the two broadening mechanisms examined, we may confidently assign Z broadening as the relevant mechanism in our experiments. A further experimental check on this assignment would be provided by the determination of the highly oriented isotactic polypropylene spectrum at cryogenic temperatures, where the crystal field splitting of the energy levels should also appear in the infrared bands, provided that sufficient spectral resolution exists.[14,15]

Summary and Comments

The fundamental results of this paper show that valence coordinate deformation processes account for the peak absorption frequency shifting with stress in highly oriented isotactic polypropylene. The observed value of the frequency-shifting coefficient α_x is expected to asymptotically approach the intrinsic value α_c with increasing sample orientation index, as the molecular stress distribution becomes increasingly uniform.

The one-dimensional anharmonic model chain may be associated with at least two independent resonance broadening mechanisms. The first arises from the presence of an average interchain perturbing force on the intrachain oscillators. The second possibility is the existence of anisotropic crystal field forces, which establish several sublevels for each principal (intrachain) quantum number. In either case, only symmetric broadening of the resonance absorption occurs for a system of uniformly stressed chains. An asymmetric wing on a stressed infrared band may therefore be associated with "overstress".

Ergun's technique[13] of solving the integral equation (2) for $F(\nu)$ verifies the frequency-shifting behavior of the original absorption bands but does not allow the sensitive determination of overstress because of the side lobes inherent in the calculational technique. Kosobukin's technique[6] will be implemented in the future to provide information on (a) the microstress level that can be sustained before bond rupture occurs and on (b) the load history that will cause sufficient bond rupture to initiate sample failure. Annealing and orientation treatments that modify the stress distribution, and hence, the sample properties, could be monitored with such a technique.

The theory[16] of one-dimensional anharmonic chains gives a linear $\alpha_c(T)$ relation for high temperature and a T^4 relation for low temperature. The experimentally determined linear $\alpha_x(T)$ relationship clearly implies that the oscillator temperature is much greater than the ambient temperature when the chains are in equilibrium with the radiation field. This is clearly inconsistent with the common interpretation of resonance broadening as due to an average interchain perturbing force. It is, however, consistent with resonance broadening by means of anisotropic, crystal field forces between chains.[11] If this interpretation is valid, then crystal field splitting could occur in the spectrum of PP obtained at cryogenic temperatures, provided, of course, that the spectral resolution of inherently overlapping bands is adequte.[14,15] At room temperature, on the other hand, broadening without splitting occurs.

The following points should be emphasized:

1. The quasi-harmonic wave functions and energies of the model chain were obtained in the stressed and unstressed conditions and verified by comparison with Morse theory.

2. The overtone transition probabilities in this model are so small compared to the fundamental transition probabilities that overtones may be completely neglected.

3. The self-energy shift was verified to be much smaller than the quasi-harmonic shift for quantum numbers $n \lesssim 10^3$ using data typical of observations on ultraoriented isotactic polypropylene. The quasi-harmonic approximation allows the integration of an anharmonic system as being harmonic but with a variable (stress and temerature dependent) spring constant. Thus there is imperceptible error in considering the energy levels to be equally spaced for $n \lesssim 10^3$.

4. An independent indication of the validity of using single-chain theory to calculate infrared frequencies is the observation[34] that although X-ray diffraction reveals three different polypropylene crystal types, their infrared spectra are essentially identical. Therefore, the infrared resonance absorption frequencies depend almost exclusively on the intrachain bonding, with negligible interchain effects at room temperature.

5. If the infrared bands are predominantly γ_0-broadened by an average interchain force, then $T_{osc} \approx T_{amb}$, and the quantum number n must be small (say, 0, 1, or 2), as verified by the calculation of the damping strength. The radiative excitation rate was calculated to be 10^{-10} or less of the nonradiative decay rate. The radiation energy absorbed by each chain is therefore very efficiently carried away ("heat sunk") to the environment by phonons. The resulting Lorentzian band is symmetric.

6. If the infrared bands are predominantly Z broadened by a random (Markovian) switching between closely spaced sublevels produced by crystal field splitting, then Kubo's analysis[11] shows that the band is symmetric. In this case $\gamma_0 \to 0$, $T_{osc} \gg T_{amb}$, and it is expected that $n = 100$ is the highest appreciably populated level. The important levels are still equally spaced in energy, but each chain is not very efficiently connected to the environment by phonons.

7. The theory of one-dimensional anharmonic chains gives $\alpha_c = -\alpha_0 - CT$ for $kT \gg \hbar\omega_0$ and $\alpha_c = -\alpha_0 - C_L T^4$ for $kT \ll \hbar\omega_0$. In these "microscopic" formulas, the T is identified with the T_{osc} seen by an individual chain in

equilibrium with the radiation field, when the sample is at the "macroscopic" ambient temperature T_{amb}. Previous data[16,22] clearly show the linear relationship; therefore $kT_{osc} \gg \hbar\omega_0 \doteq 0.145$ eV $> kT_{amb}$, where kT_{amb} for the data ranges from 0.017 to 0.034 eV. This is only possible for the Z-broadening mechanism, which arises from transitions between crystal field sublevels of each quantum number n. The validity of this mechanism can be further checked experimentally by determining whether or not the crystalline peaks in Figure 1 show splitting at cryogenic temperatures.[32]

8. The above observations imply that the presence of a uniform stress level in highly oriented isotactic polypropylene can be modeled by one-dimensional anharmonic chains subject to the Z-broadening mechanism. The only way known at present to account for the asymmetric wings seen in Figures 2 and 3 is to attribute them to a distribution of elementary oscillators among different stress levels. As more refined methods of deconvolution are implemented, the molecular stress distribution analysis is expected to furnish valuable new information about the load-bearing capabilities of polymers.

9. Kubo's broadening theory may apply to other spectroscopic problems beyond the scope of this paper. For example, Zerbi et al.[35] have shown that a submelting point transition at 22.8 °C from orthorhombic to "α" n-nonadecane is consistent with the onset of a particular motion of the molecules while still in the solid state. The main outcome of each of three schools of thought is that paraffin chains are able to slide out of the crystal core by rototranslational motion. While it is certainly true, upon reaching the 32 °C melting point, that all the chains must have "slipped out" of the lamellae (which no longer exist), Kubo's analysis may call into question the interpretation that the orthorhombic lattice is mostly destroyed at the 22.8 °C phase transition. There, the 2.5% increase in volume could reduce the orthorhombic crystal field interaction forces, increase the sublevel switching rate, and eliminate the spectroscopic effects (e.g., 720/730 splitting) of the orthorhombic crystal field before the structure itself is destroyed. In fact, X-ray evidence[36] is compatible with the choice of an orthorhombic unit cell in the α phase. These considerations do not, of course, affect the conclusion of the rototranslational motion of the chains out of the lamellae, which could occur above 22.8 °C without requiring the immediate transformation into a nonorthorhombic structure.

10. Interpretations of frequency shifts in stressed polypropylene are consistent with recent Raman and infrared studies of frequency shifts in highly oriented polyethylene.[37] The 1063- and 1130-cm^{-1} carbon–carbon skeletal mode bands exhibit large frequency shifts with stress.

Acknowledgment. We are grateful to the National Science Foundation's Polymer Program for financial support of this work, Grant DMR 82-16181.

Registry No. Isotactic polypropylene (homopolymer), 25085-53-4; polyethylene (homopolymer), 9002-88-4.

References and Notes

(1) R. P. Wool, *J. Polym. Sci., Polym. Phys. Ed.*, **13**, 1795 (1975).
(2) R. P. Wool, *Polym. Eng. Sci.*, **20**, 805 (1980).
(3) R. P. Wool and R. H. Boyd, *J. Appl. Phys.*, **51**, 5116 (1980).
(4) G. Zerbi, L. Piseri, and F. Cabassi, *Mol. Phys.*, **22**, 241 (1971).
(5) R. P. Wool, *J. Polym. Sci., Polym. Phys. Ed.*, **14**, 1921 (1976).
(6) V. A. Kosobukin, *Sov. Phys.—Solid State (Engl. Transl.)*, **14**, 2246 (1973).
(7) R. P. Wool, *J. Polym. Sci., Polym. Phys. Ed.*, **19** 449 (1981).
(8) S. N. Zhurkov, V. I. *Vettegren*, V. E. Korsukov, and I. I. Novak, *Sov. Phys.—Solid State (Engl. Transl.)*, **11**, 233 (1969).
(9) D. K. Roylance and K. L. DeVries, *J. Polym. Sci., Part B*, **9**, 443 (1971).
(10) V. A. Kosobukin, *Opt. Spectrosc.*, **34**, 154 (1973).
(11) R. Kubo, in "Fluctuation, Relaxation and Resonance in Magnetic Systems", D. ter Haar, Ed., Plenum Press, New York, 1962.
(12) C. R. Desper, *J. Macromol. Sci., Phys.*, **B7**, 105 (1973).
(13) S. Ergun, *J. Appl. Crystallogr.*, **1**, 19 (1968).
(14) J. K. Kauppinen, D. J. Moffatt, H. H. Mantsch, and D. G. Cameron, *Appl. Spectrosc.*, **35**, 271 (1981).
(15) J. K. Kauppinen, D. J. Moffatt, D. G. Cameron, and H. H. Mantsch, *Appl. Opt.*, **20**, 1866 (1981).
(16) R. S. Bretzlaff and R. P. Wool, *J. Appl. Phys.*, **52**, 5964 (1981).
(17) Y.-L. Lee, R. S. Bretzlaff, and R. P. Wool, *J. Polym. Sci., Polym. Phys. Ed.*, in press.
(18) The calculation of the thermodynamic quantities could proceed without the weak-coupling assumption. If all the bonds in the model one-dimensional chain were equally strong, there would be a monatomic basis, with the calculation proceeding as in ref 19. The weak-coupling assumption only reflects the results of ref 3, where the ratio $\Delta R{:}\Delta\theta{:}\Delta\phi$ = C–C stretching:valence angle bending:torsional angle expansion was calculated to be 1:2.4:9 for a polypropylene helix. Part of the molecule is appreciably weaker than the remainder. The appropriate one-dimensional model is therefore a weakly coupled, diatomic chain, as in ref 16. Of course, the model must be at least diatomic if there are to be any optical branches to the dispersion curves. The Einstein approximation ($\omega(k)$ = constant) for the optical branches is tacitly assumed in eq 8 of ref 16. An equivalence of all $\omega(k)$ is necessary to derive eq 13c in ref 16 (eq 22a in this work).
(19) G. Leibfried and W. Ludwig, *Solid State Phys.*, **12**, 276 (1961).
(20) R. A. Cowley, *Adv. Phys.*, **12**, 421 (1963).
(21) R. S. Bretzlaff, M.S. Thesis, University of Illinois, Urbana, 1980.
(22) S. K. Upadhyayula, M.S. Thesis, University of Illinois, Urbana, 1980.
(23) P. M. Morse and H. Feshbach, "Methods of Theoretical Physics", McGraw-Hill, New York, 1953, p 1162.
(24) D. Park, "Introduction to the Quantum Theory", McGraw-Hill, New York, 1964, pp 228–229.
(25) P. M. Morse, *Phys. Rev.*, **34**, 57 (1929).
(26) M. Sargent, M. O. Scully, and W. E. Lamb, "Laser Physics", Addison-Wesley, Reading, MA, 1974, Chapter 8.
(27) A. Einstein, *Phys. Z.*, **18**, 121 (1917).
(28) J. D. Jackson, "Classical Electrodynamics", Wiley, New York, 1962, p 498.
(29) L. I. Schiff, "Quantum Mechanics", McGraw-Hill, New York, 1968, p 405.
(30) C. Nakafuku, *Polymer*, **19**, 149 (1978).
(31) M. Tasumi and T. Shimanouchi, *J. Chem. Phys.*, **43**, 1245 (1965).
(32) R. S. Bretzlaff and R. P. Wool, work in progress.
(33) N. W. Ashcroft and N. D. Mermin, "Solid State Physics", Holt, Rinehart, and Winston, New York, 1976, p 457.
(34) G. F. Trott, *J. Appl. Polym. Sci.*, **14**, 2421 (1970).
(35) G. Zerbi, R. Magni, M. Gussoni, K. Holland-Moritz, A. Bigotto, and S. Dirlikov, *J. Chem. Phys.*, **75**, 3175 (1981).
(36) K. Larsson, *Nature (London)*, **213**, 383 (1967).
(37) R. P. Wool, R. S. Bretzlaff, B.-Y. Lee, C. H. Wang, and R. H. Boyd, results to be published.